This is the author's version of an article that has been published in this journal. Changes were made to this version by the publisher prior to publication.
The final version of record is available at http://dx.doi.org/10.1109/TPEL.2013.2292600

Modulated Ramp PWM Generator for Linear Control of the Boost Converter's Power Stage

Vratislav Michal

ST-Ericsson and CPE Lyon, 12 rue Jules Horowitz, 38000, Grenoble - France. vratislav.michal@st.com,

Abstract — In this paper, the concept of the modulated-ramp PWM generator is presented. The specific nonlinear behavior of this generator enables an exact linear control-to-output static conversion characteristic of DC-DC switching converters, such as the boost (step-up), buck/boost, Ćuk or Sepic, operating in Continuous Conduction Mode (CCM). The resulting linearization leads to a significant improvement of the control accuracy, and simplification of the converters, operating mainly in the open-loop architecture. In this paper, the concept of the modulated-ramp PWM generator is described, followed by a detailed steady-state and small-signal AC analysis. The key aspects for practical implementation are also highlighted. All results and benefits of the modulated-ramp PWM generator are demonstrated here on the boost converter power stage.

Index Terms—modulated ramp PWM generator, linear control-to-output transfer function, SMPS boost converter.

I. INTRODUCTION

The conventional realization of switched-mode power converters such as boost, buck-boost, Ćuk or SEPIC suffers from significant nonlinearity of the control-to-output transfer function [1], [2]. The nonlinearity is manifested mainly by a significant variation of the control gain GC. As a consequence, specific nonlinear control schemes are frequently used for booth open loop or closed loop converter architectures.

The basic scheme of a boost converter power stage is shown in *Fig. 1*. It consists of a voltage source V_{IN}, a switch SW including parasitic resistances R_{SW}, an LC filter with parasitic elements R_L and R_{ESR}, a load resistance R, and a conventional (linear) pulse-width modulator (PWM). In Continuous Conduction Mode (CCM), the static input-to-output conversion ratio V_{OUT}/V_{IN} for the ideal converter ($R_L = R_{SW} = 0$) is usually determined from equal positive and negative inductor current increments $\Delta I_{L1,ON} = \Delta I_{L1,ON}$ occurring during the ON and OFF switching phases [1], [2], [3] as:

$$\frac{V_{OUT}}{V_{IN}} = \frac{1}{1-D} \tag{1}$$

where D is the duty-cycle ratio. The small-signal control gain G_C relating to the incremental gain at the operating point (steady-state output voltage) can be obtained from (1) as the partial derivative:

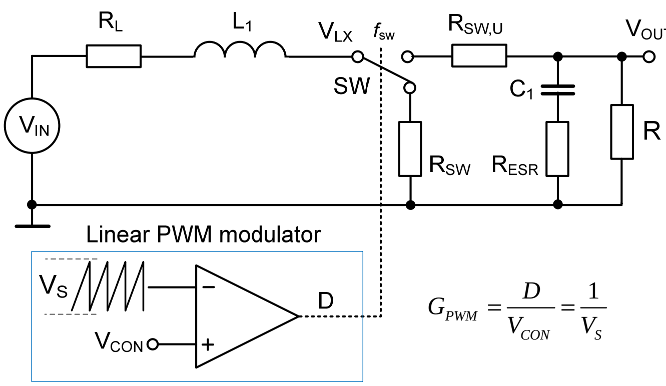

Fig. 1. Basic scheme of a boost converter power stage.

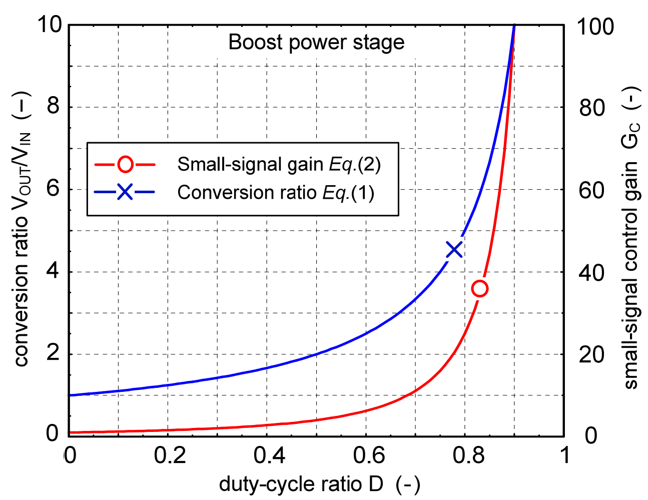

Fig. 2. Conversion ratio V_{OUT}/V_{IN} and small-signal control gain G_C of the ideal boost converter for $V_{IN} = 1$.

$$G_C = \left.\frac{\partial V_{OUT}}{\partial D}\right|_{V_{IN}=const} = \frac{V_{IN}}{(1-D)^2} \tag{2}$$

This expression is highly non-linear. As we can observe from the graphical interpretation of (2) shown in *Fig. 2*, the usual duty-cycle range ($D < 0.9$) causes high variation of the small-signal control gain G_C, even up to 40dB. This means that an incremental ΔD at high duty cycle ratio will cause significantly higher (up to 100-times) variation of V_{OUT}, compared to the identical increment ΔD applied at low duty-cycle ratio. In the open loop architecture, this nonlinearity decreases the conversion ratio accuracy (1) due to increased sensitivity, whereas in the closed loop architecture, it can affect the stability of the converter. In addition, another nonlinearity caused by the non-ideal components is encountered in the analysis of the converter. As we will show later, this involves mainly the parasitic resistances of the inductor and switch, and is manifested by the negative control gain G_C at high duty-cycle (see *Fig. 9*) [1].

In the domain of the feedback control, a lot has been done to address the problem of nonlinear control-to-output conversion. The closed-loop transfer function design in voltage control mode is usually based on the linearization around an operating point [3], [4], [5], or by using feedback linearization [6], [7].

A more suitable way is the predistortion technique which allows linearization of the static conversion ratio control through the specific PWM modulator schemes. Basically, predistortion can either be applied to the control signal [8] or to the voltage ramp [9]. However,

common problems of these techniques are the increased modulator complexity, and low accuracy of generated duty-cycle. We can refer for example to [8], where the error signal used for the predistortion is obtained by the filtering of the output PWM signal waveform. An analysis of this technique reveals a high sensitivity to the power-supply voltage (PWM signal peak amplitude), and to the delay caused by the filtering of the PWM signal, where several clock periods are required to obtain properly filtered error signal.

In this paper, a concept based on the predistortion by modulated-ramp PWM generator is presented. The result shows that a linear relationship between control variable and output voltage is obtained. The achieved linear control characteristic yields considerably lower sensitivities, compared to the conventional linear PWM modulator, namely for high duty-cycle values (D > 0.5). This feature can allow to avoid the use of the closed-loop architecture, resulting in a simpler open-loop architecture of the power converter. This simplification can be done in cases where the constraints of the output voltage accuracy are low, such as the power supply of RF PA, LED drivers, battery chargers etc. Concept of modulated-ramp PWM generator can also be used in the closed loop architecture (current or voltage mode), where, as shown in the following, the nonlinear dynamic behavior of the power stage has to be considered.

This article is organized as follows: in *section II*, the concept of a current-modulated ramp PWM generator is presented, with an emphasis on the fundamental relationships between the input control value (control current I_{CON}), duty-cycle *D*, and boost converter output voltage V_{OUT}. *Section III* presents a detailed analysis of the modulated-ramp boost converter, while *section IV* deals with basic implementation constraints and shows an experimental result.

I. Current-Modulated Ramp PWM Generator

The conventional "linear" PWM generator is depicted in *Fig. 3*. As we can see, it consists of a constant voltage ramp generator, comparator, and control input $V_{CON}(t)$. The constant voltage ramp is obtained thanks to a DC bias current I_b injected into the periodically discharged capacitor *C*. This type of PWM generator yields a constant control-voltage to duty-cycle gain $1/V_m$ (V_m is the voltage ramp amplitude and is further considered unitary). Hence, use of this generator preserves the nonlinear conversion characteristic V_{OUT}/V_{IN} and DC control gain G_C, given by *Eqs*. (1) and (2).

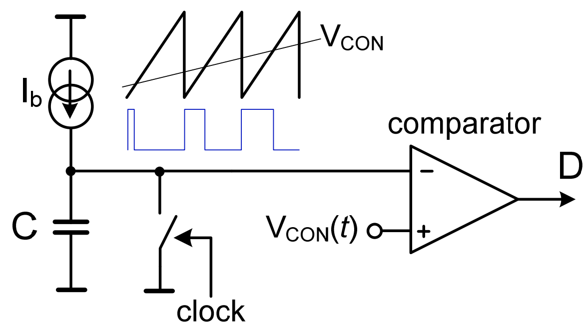

Fig. 3. Model of conventional (linear) PWM generator composed of a constant current source I_b, periodically discharged capacitor, and comparator.

A. Current-modulated Ramp PWM Generator

The permutation of the control and reference inputs (I_b and V_{CON}) in the original circuit from *Fig. 3* results in a suitable nonlinear behavior of the generator. This modification creates the generator PWM with modulated voltage ramp, which is shown in *Fig. 4*. Here, the input variable is the control current $I_{CON}(t)$, whereas the comparator input voltage V_b remains constant.

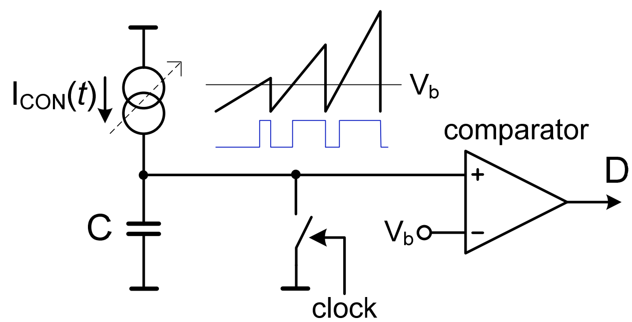

Fig. 4. Current-modulated ramp PWM generator. $I_{CON}(t)$ is the input control variable and V_b is the constant bias voltage.

The control-to-duty-cycle conversion ratio of the modulator shown in *Fig. 4* can be determined from a time analysis of the capacitor voltage $V_C(t)$. When considering, for convenience, the control current I_{CON} constant during one clock period *T*, the capacitor voltage $V_C(t)$ results in a linear time function of I_{CON}:

$$V_C(t) = \frac{1}{C}\int_T I_{CON}(t)dt \approx \frac{I_{CON}}{C}t \tag{3}$$

As shown in *Fig. 4*, capacitor voltage is compared with an arbitrary reference voltage V_b. While $V_C < V_b$, the output of the PWM modulator is low. $V_C(t)$ reaches the value V_b at $t = V_b C / I_{CON}$, at which time the output of the modulator goes high. Considering the capacitor being discharged with period *T*, the duty-cycle ratio D can be expressed as:

$$D = 1 - \frac{V_b C}{I_{CON} T} = 1 - \frac{\alpha}{I_{CON}} \tag{4}$$

which is defined for $I_{CON(min)} > V_b \cdot C/T$. A demonstration for two

This is the author's version of an article that has been published in this journal. Changes were made to this version by the publisher prior to publication.
The final version of record is available at http://dx.doi.org/10.1109/TPEL.2013.2292600

discrete values of control current I_{CON1} and I_{CON2} is shown in *Fig. 5*, where it can be seen how the slope of $V_C(t)$ varies with the control current.

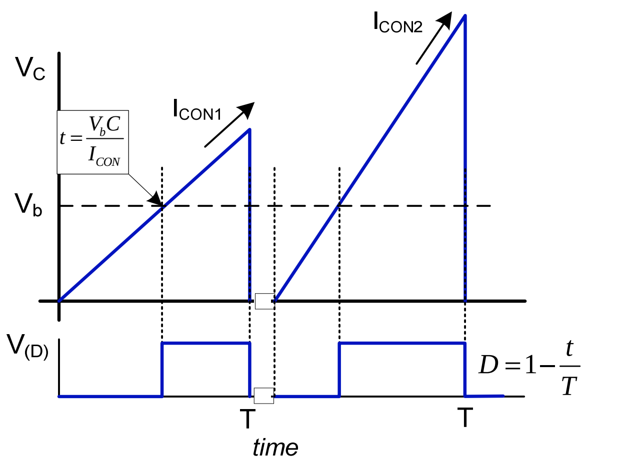

Fig. 5. Capacitor voltage $V_C(t)$ for two different values of I_{CON1} and I_{CON2} (I_{CON1} and I_{CON2} are considered constant within the clock period).

B. *Demonstration on the Step-Up Converter*

The obtained relationship (4) between duty-cycle D and control current I_{CON} can be substituted in the boost converter conversion ratio *Eq.* (1). The resulting dependency is a linear function of I_{CON}:

$$\frac{V_{OUT}}{V_{IN}} = \frac{I_{CON} T}{V_b C} \tag{5}$$

and is defined for $I_{CON} > I_{CON(min)}$. Small-signal control gain G_C can be obtained from (5) as a constant term:

$$G_C = \left.\frac{\partial V_{OUT}}{\partial I_{CON}}\right|_{V_{IN}=const} = \frac{V_{IN} T}{V_b C} \tag{6}$$

This means that, contrary to (2), an arbitrarily small step ΔI_{CON} causes an identical step ΔV_{OUT}, independent on the steady-state output voltage. Similar to the boost-converter power stage, conversion characteristics and small-signal control gain for other mentioned converters can be obtained. As we can see in *Table 1* below, the boost, buck/boost, Ćuk, and SEPIC DC/DC converters with modulated-ramp PWM generator exhibit linear V_{OUT}/V_{IN} conversion characteristic and a constant small-signal gain G_C.

C. *Switched-simulation Example*

The technique presented above for the linearization of the static conversion characteristic is demonstrated here by the slow (*i.e.* quasi-static) switched transient simulation of an ideal boost converter power stage. The simulation setup is shown in *Fig. 6*. In this model, the excitations (control values V_{CON} and I_{CON}) are realised: *i*) for the linear PWM generator by a 40ms voltage ramp from 0 to 1V, and *ii*) for the modulated ramp PWM by a 40ms current ramp from 1.6µA to 16µA. The resulting time responses are shown in *Fig. 7*, where the linear control to output conversion for modulated ramp PWM generator can be observed.

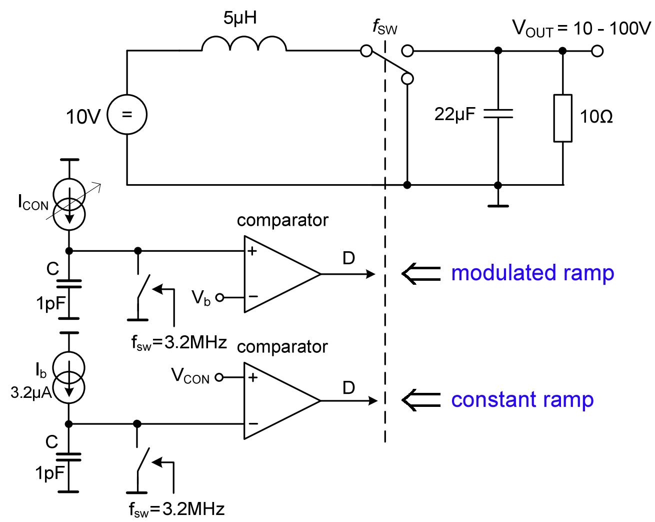

Fig. 6. Switched-simulation scheme of boost converter with linear (Fig. 3) and modulated ramp (Fig. 4) PWM generators.

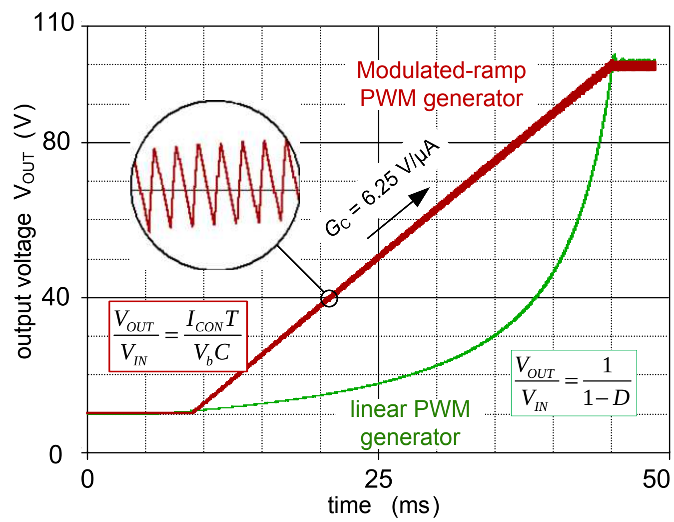

Fig. 7. Switched transient simulation of *Fig. 6* boost converter with linear (*Fig. 3*) and modulated-ramp (*Fig. 4*) PWM generators (duty-cycle is linearly increasing with time).

II. DC AND AC CHARACTERISTICS OF THE MODULATED-RAMP BOOST SWITCHED CONVERTER

The boost power converter with modulated-ramp PWM generator exhibits constant V_{OUT}/I_{CON} conversion gain. However, the parasitic elements in the circuit (mainly the inductor's series resistance R_L, see *Fig. 1*) introduce extra higher-order terms to transfer characteristics.

Due consideration for these parasitics is important for the proper design of the system, and is the matter of the following paragraph. Here, the comparison of non-ideal boost converter DC and AC characteristics is provided between the conventional linear (*Fig. 3*), and modulated-ramp PWM generators (*Fig. 4*).

TABLE I

This is the author's version of an article that has been published in this journal. Changes were made to this version by the publisher prior to publication.
The final version of record is available at http://dx.doi.org/10.1109/TPEL.2013.2292600

CONVERSION RATIO V_{OUT}/V_{IN} AND CONTROL GAIN G_C OF BASIC POWER STAGES OPERATING IN CCM

	Linear PWM	**Modulated-ramp PWM**	
Power stage	conversion ratio V_{OUT}/V_{IN}	conversion ratio V_{OUT}/V_{IN}	control gain G_C
Boost	$\frac{1}{1-D}$	$\frac{I_{CON}T}{V_b C}$	$\frac{V_{IN}T}{V_b C}$
Buck/Boost - Ćuk	$-\frac{D}{1-D}$	$1-\frac{I_{CON}T}{V_b C}$	$-\frac{V_{IN}T}{V_b C}$
Sepic	$\frac{D}{1-D}$	$\frac{I_{CON}T}{V_b C}-1$	$\frac{V_{IN}T}{V_b C}$
Buck	D	$1-\frac{V_{bias}C}{I_{CON}T}$	$\frac{V_{IN}V_b C}{I^2_{CON}T}$

A. Small-signal Model of the Boost Converter

The inherent nonlinear behaviour of the switches is treated in widely available literature, providing methods which allow linear (small-signal) representation of switched converters.

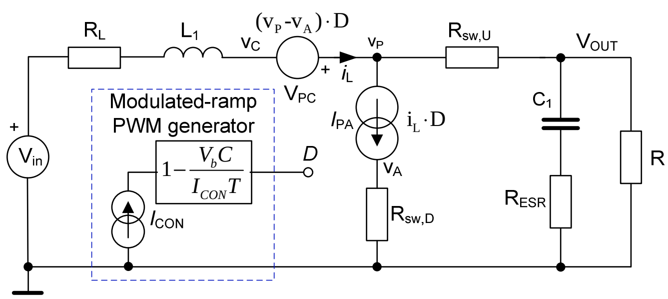

Fig. 8. Linear model of boost converter power stage. V_{PC} and I_{PA} forms the "DC transformer" [2]. In following, we consider: $V_{in} = 10$V, $L_1 = 5\mu$H, $C_1 = 22\mu$F, $R_L = 150$mΩ, $R_{ESR} = 20$mΩ, $R = 100\Omega$ $V_b = 0.5$V, $C = 1$pF, $T = 0.3125\mu$s ($\alpha = 1.6\mu$A), $R_{swU,D} = 0$.

Generally, approaches to the linear representation are based on averaging, provided either in the state-space (State Space Averaging - SSA) [2], [10] or through the averaged switch model [12] (sometimes presented as "DC transformer" [2]). The advantage of the averaged switch model is its compatibility with circuit simulation environments. The model of the boost DC/DC converter shown in *Fig. 8*, which is based on this concept, is described *e.g.* in [2]. Here, the dependent sources V_{PC} and I_{PA} represent the average voltage and current of the switch terminals (averaged over one clock period), variable D is the duty-cycle, and the rectangle representing *Eq.* (4) embodies the modulated ramp PWM generator. The switches' resistance R_{sw} in *Fig. 8* model are shown for convenience and are not considered in the following. (An efficient method to embody the nonlinear resistance of semiconductor switches is presented in [14]). Generally, the accuracy of AC simulation with the given averaged models decreases at frequencies approaching the switching frequency [1], [11]. This is to be considered in the evaluation of the following AC characteristics, where the switching frequency is not specified.

B. Static V_{OUT}/V_{IN} Conversion Characteristics

The steady-state analysis of *Fig. 8's* circuit model leads to an improvement in the accuracy of V_{OUT}/V_{IN} conversion ratio (5). We focus on higher order terms which cause the spurious drop of V_{OUT} towards zero at high duty-cycle [1]. Beyond the excessive increase of the inductor and switch currents, the high duty cycle value (above D_{MAX}, *see Fig. 9*) causes the inversion of the control gain polarity, which can affect the stability of the converter operating in closed-loop. In practical applications, a positive control gain G_C is usually maintained by employing an advanced control technique, such as current-mode control [1], [10], [13]. In such techniques, the inductor current I_L is measured and limited to a certain value (below D_{MAX}) by an additional current-sensing circuit. However, an accurate current sensing circuit may be difficult to integrate at high switching frequencies, which limits the maximum switching frequency of the converter [15]. Compared to linear PWM schemes (*Fig. 3*), the modulated-ramp PWM generator shown in *Fig. 4* provides a method to maintain a positive small-signal control gain G_C, and limits the maximal current I_L by the natural limitation of the duty-cycle, via the maximal value of I_{CON}.

The V_{OUT}/V_{IN} conversion ratio of a boost converter power stage with linear PWM modulator containing parasitic resistance R_L can be derived from *Fig. 8* model as:

$$V_{OUT} = \frac{V_{IN}}{1-D+\frac{R_L}{R\,(1-D)}} \qquad (7)$$

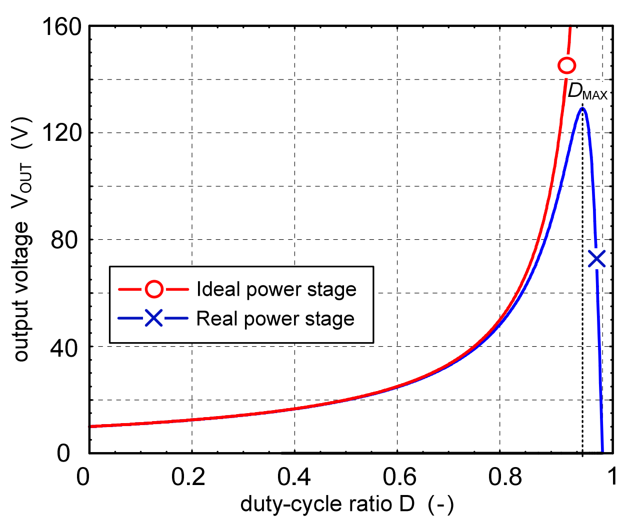

Fig. 9. Comparison of real ($R_L = 150$ mΩ) and ideal ($R_L = 0$) conversion characteristics of boost converter with linear PWM generator and load resistance $R = 100\ \Omega$.

which, for the ideal case ($R_L \rightarrow 0$) converges to (1). An example of the conversion characteristic (7) for real ($R_L > 0$) and ideal ($R_L = 0$) power stages are shown in *Fig. 9*. Here we notice the mentioned point D_{MAX} ($dV_{OUT}/dD = 0$) where the control gain G_C changes the polarity.

In comparison, the boost converter power stage with modulated-ramp PWM generator can be described by the static conversion ratio:

$$V_{OUT} = \frac{V_{IN}}{\alpha + \frac{R_L}{\alpha R} I_{CON}^2} I_{CON} \tag{8}$$

For low control current values, this approximates a linear function of I_{CON} (*Fig. 10*). The maximum allowed control current $I_{CON(max)}$ which corresponds to the value where the PWM generator produces the duty-cycle value D_{MAX} results from (8) as:

$$I_{CON\,(\max)} = \sqrt{\frac{R}{R_L}} \cdot \frac{V_b C}{T} = \alpha \sqrt{\frac{R}{R_L}} \tag{9}$$

As an illustration of *Eq.* (9), we can refer to a power stage with parameters listed in the caption of *Fig. 8*. This power stage exhibits the point $dV_{OUT}/dI_{CON} = 0$ at $I_{CON(max)} = 41$ µA. As we can see from the conversion characteristic shown in *Fig. 10*, this point is far from the considered dynamics of I_{CON}, being between 1.6µA and 14µA (conversion ratio V_{OUT}/V_{IN} from 1 to 8). For a safe choice of maximal control current value I_{MAX}, we can mention the expression of the maximal inductor current I_{Lmax} [3] (D_{max}, I_{max} refers to the maximal values defined by design):

$$I_{L\,max} = \frac{V_{OUT}}{R\left(1 - D_{max}\right)} = \frac{V_{OUT} I_{max}}{\alpha R} \tag{10}$$

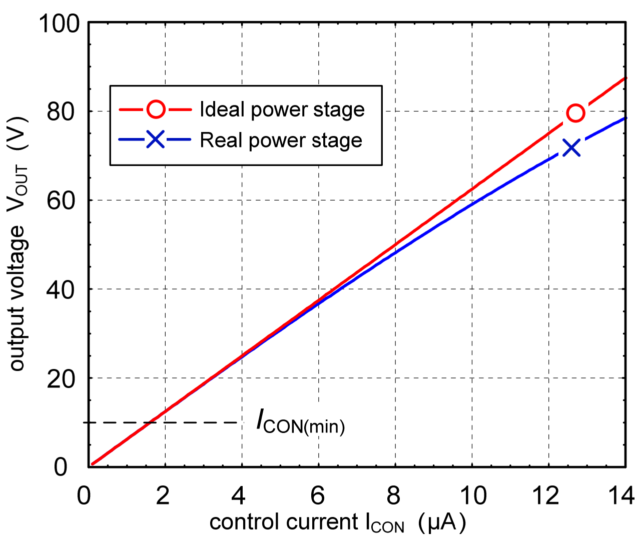

Fig. 10. Comparison of real ($R_L = 150$ mΩ) and ideal ($R_L = 0$) boost converter conversion characteristics with modulated-ramp PWM generator (parameters of the simulation are listed in *Fig. 8* caption)

C. Control-to-Output Transfer Function

The dynamic behavior of the boost converter power stage with modulated-ramp PWM generator can be described by appropriate transfer functions. We focus here on the control-to-output transfer function $G_C(s) = V_{OUT}(s)/I_{CON}(s)$, which is compared to the transfer function $V_{OUT}(s)/D(s)$. Additional frequency characteristics, such as line susceptibility or output impedance are identical for both PWM generators, and can be found *e.g.* in refs. [10], [13].

The transfer function $G_C(s)$ is obtained by the linearization of the converter around an operation point (I_{CON} or D, V_{IN}, I_L and V_{OUT}). Thus, AC analysis of the circuit in *Fig. 8* requires first a steady-state analysis, in order to determine the gain of the dependent sources V_{PC} and I_{PA}. For the purpose of AC analysis, the dependent sources V_{PC} and I_{PA} in *Fig. 8* model are defined as follows (we neglect $R_{SWU,D}$): $V_{PA} = v_{OUT}{\cdot}D + V_{OUT}{\cdot}d$ and $I_{PA} = i_L{\cdot}D + I_L{\cdot}d$. Here V_{OUT}, I_L and D are the steady-state (constant) values (7), (8), (10), v_{OUT} and i_L are the AC values, and d is the AC control input.

An analysis of the linear model of *Fig. 8* results in the transfer function $G_C(s)$ for a modulated ramp and linear PWM generator as $V_{OUT}(s)/I_{CON}(s)$ and $V_{OUT}(s)/D(s)$, respectively. Both transfer functions can be expressed in the following polynomial form:

$$G_C(s) = G_C \frac{\left(1 + \frac{s}{z_1}\right)\left(1 - \frac{s}{z_2}\right)}{\frac{1}{\Omega_0^2}\left(s^2 + \frac{\Omega_0}{Q} s + \Omega_0^2\right)} \tag{11}$$

where z_1 is the left and z_2 right half-plane real zero frequencies, Q is the quality factor, and Ω_0 the resonant frequency of the 2nd order denominator polynomial. The coefficients corresponding to the transfer function of power stages with both types of PWM modulators are listed in *Tab. II*.

TABLE II

COEFFICIENTS OF THE CONTROL-TO-OUTPUT TRANSFER FUNCTION (11)

Coef	Linear PWM generator	Modulated-ramp PWM generator
z_1	$\frac{1}{R_{ESR} C_1}$	$\frac{1}{R_{ESR} C_1}$
z_2	$\frac{R(1-D)^2 - R_L}{L_1}$	$\frac{1}{L_1}\left(\frac{\alpha^2 R}{I_{CON}^2} - R_L\right)$
Ω_0	$\sqrt{\frac{R_L + R\left(1-D\right)^2}{L_1 C_1 \left(R_{ESR} + R\right)}}$	$\sqrt{\frac{\alpha^2 R / I_{CON}^2 + R_L}{L_1 C_1 \left(R + R_{ESR}\right)}}$
Q	$\frac{\Omega_0 L_1 C_1 \left(R + R_{ESR}\right)}{C_1 R\left(R_{ESR}\left(1-D\right)^2 + R_L\right) + L_1}$	$\frac{\Omega_0 L_1 C_1 \left(R_{ESR} + R\right)}{C_1 R\left(R_{ESR}\left(\frac{\alpha}{I_{CON}}\right)^2 + R_L\right) + L_1}$

The DC control gain G_C in *Eq.* (11), which in the ideal case was given by *Eqs.* (2) and (6), can now be derived for the linear PWM generator from the V_{OUT}/V_{IN} conversion characteristic (7) as:

$$G_C = \left.\frac{\partial V_{OUT}}{\partial D}\right|_{V_{IN}=const} = \frac{\left(1-D\right)^2 - R_L/R}{\left(R\left(1-D\right)^2 + R_L/R\right)^2} V_{IN} \tag{12}$$

and for the modulated ramp PWM generator from (8) as:

This is the author's version of an article that has been published in this journal. Changes were made to this version by the publisher prior to publication.
The final version of record is available at http://dx.doi.org/10.1109/TPEL.2013.2292600

$$G_C = \left.\frac{\partial V_{OUT}}{\partial I_{CON}}\right|_{V_{IN}=const} = \frac{V_{IN}}{\alpha}\frac{1-\frac{R_L I_{CON}^2}{\alpha^2 R}}{\left(1+\frac{R_L I_{CON}^2}{\alpha^2 R}\right)^2} \tag{13}$$

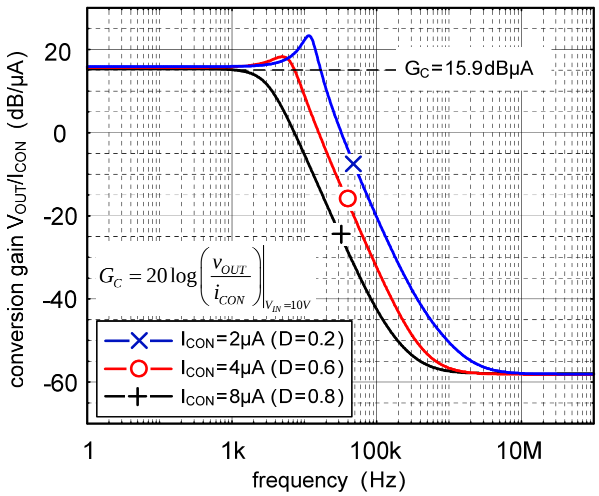

Fig. 11. Control-to-Output transfer functions of modulated-ramp boost converter (parameters of the simulation are listed in *Fig. 8* caption).

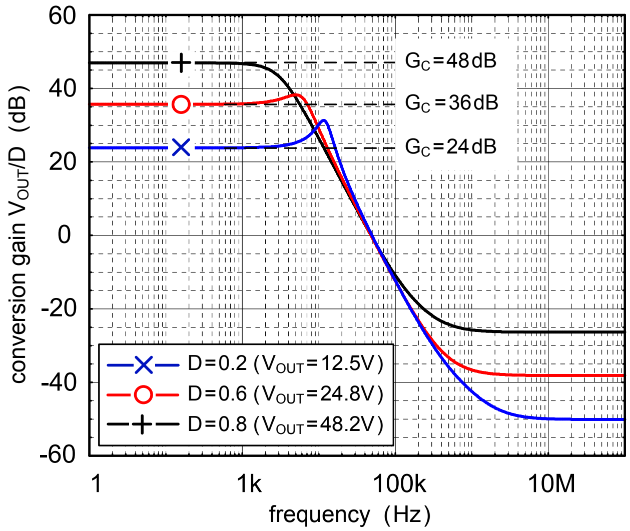

Fig. 12. Control-to-output transfer functions for three duty-cycle values. (parameters of the simulation are listed in *Fig. 8* caption).

The first term V_{IN}/α In equation (13) is the ideal DC small signal gain as in (6), and the term containing I_{CON} is the term responsible for the parasitic nonlinear behaviour (see *Fig. 10*).

A graphical representation of the transfer function (11) for the boost-converter with modulated-ramp PWM generator is shown in *Fig. 11*. In this figure, bode plots corresponding to three discrete values of the control current I_{CON} are shown. We notice the expected very low variation of the DC control gain given by *Eq.* (13), and variation of coefficients z_2, Ω_0 and Q, which is in line with terms shown in *Tab. II*.

Compared to this, the boost converter with conventional linear PWM generator exhibits a control gain variation in the order of 24dB (for identical conversion ratios V_{OUT}/V_{IN} as in *Fig. 11*). This is graphically shown in *Fig. 12*.

III. Implementation Considerations and Experimental Results

As shown in *Fig. 3*, the modulated-ramp PWM generator requires the integration of the controlled current source I_{CON}, comparator, and a constant bias voltage source V_b. As follows from *Eq.* (5), the bias voltage V_b can be used to adjust the control gain, if necessary.

For very low V_b, the control current I_{CON} can be obtained directly from a control voltage by a large value series resistance (RC integrator). In other cases, an active current source may be used, in order to achieve linear conversion $V_{CON} \rightarrow I_{CON}$. Two examples are the non-inverting Howland current source [16] and the current conveyor (CCII+) based circuit shown in *Fig. 13* [17]. In the circuit shown in *Fig. 13*, the conversion transconductance is simply given by $I_{CON} = V_{CON}/R$.

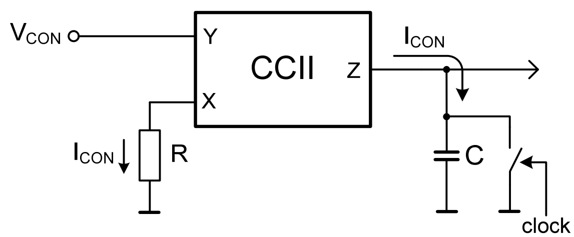

Fig. 13. Single ended current source based on the second-generation CC [17].

Alternatively, a very simple realization can be achieved by using the inverting integrator shown in *Fig. 14*. Except for the inversion property of this circuit (inverted V_{CON}), the benefit from the low output impedance of the output node is that it allows the elimination of parasitic load capacitance.

It should also be noted that most of today's PWM generators use the triangular wave generated PWM [18] rather than this one, based on the sawtooth-wave ramp. This avoids excessive current during the discharging of the integrating capacitor. The presented technique of modulated ramp PWM can be adapted to the modulated triangle-wave amplitude, which extends the possible application of the presented linearization technique.

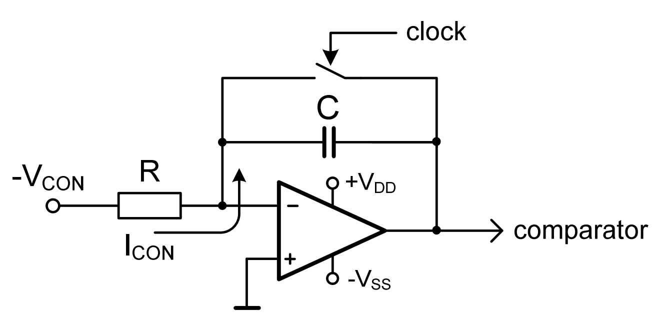

Fig. 14. Inverting modulated-ramp PWM generator. Generated ramp is available on the operation amplifier output.

In a closed-loop control scheme, the current I_{CON} can be generated directly by the controller with the current output terminal. For example, an active current-output derivative-filtered PID controller is shown in *Fig. 14*, based on a grounded RLC circuit. The grounded inductor L forms the integrator, R_1 is related to the proportional gain and R_2C_2 to the filtered derivative component of the controller transfer function [19].

The inductorless circuit equivalent to *Fig. 15* can be obtained by topological transformation. One realization of the active circuit based on an operational amplifier is shown in *Fig. 16*, where the lossy grounded inductor is realized by R_3C_3 and operational amplifier [20], C_2R_2 corresponds approximately to the derivative branch of *Fig. 15* circuit (with identical values), and voltage divider R_H and R_L steps down the output voltage to the reference voltage level.

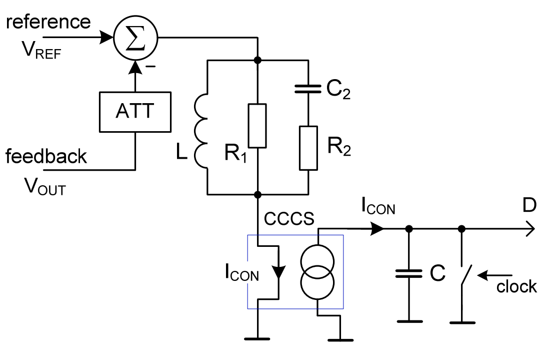

Fig. 15. Behavioral model of the current-output derivative-filtered PID controller with CCCS (current-controlled current source).

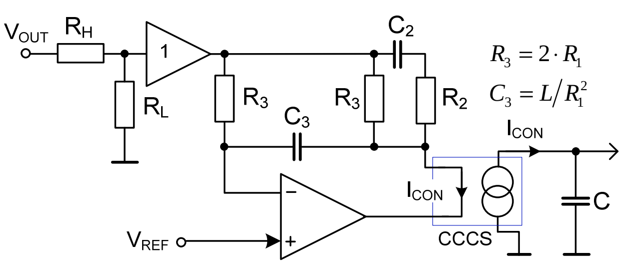

Fig. 16. Active equivalent of Fig. 15 current-output PID controller. (R3 = 462kΩ, C3 = 185pF, R2 = 9.3kΩ C2 = 45pF, RH = 19 kΩ, R = 1 kΩ).

The set of values shown in *Fig. 16* were computed to stabilize the converter model from *Fig. 8* with reference gain $V_{OUT}/V_{REF} = 20$ (L = 9.85H, R_1 = 231kΩ, R_2 = 9.3kΩ, C_2 = 45pF). The operational amplifier output current can be measured by sensing the bias current as shown in *e.g.* in [17].

IV Measured Example

A practical benefit from the use of the modulated-ramp PWM generator is shown here by measurement of a boost converter power stage. In the experiments, the PWM modulator uses the scheme from Fig. 6 with C = 71pF (including parasitic capacitances), and clock frequency fsw = 500kHz. The power stage is built using an N-channel power MOSFET transistor with low RDSON < 100mΩ and a Schottky diode rectifier. The 0.5V bias voltage Vb results in α = VbC/T = 17.7×10−6 (6), which gives a control current range of 30 − 150µA (conversion ratio from 1 to 8).

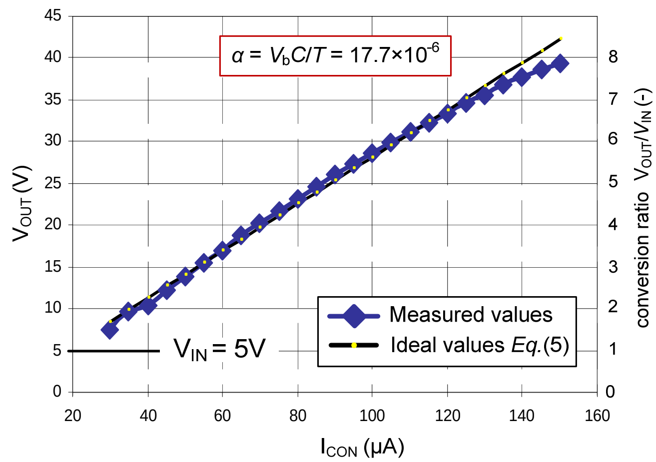

Fig. 17. Measured steady-state output voltage and conversion ration V_{OUT}/V_{IN} of the boost converter with modulated-ramp PWM generator, comparison with ideal characteristic *Eq.* (5) (V_{IN} = 5V, f_{SW} = 500kHz, C = 71pF, L = 10µH, C_1 = 22µF, R = 120Ω).

The comparison of measured output voltage and output voltage calculated per *Eq.* (5) is shown in *Fig. 17*. We can see the low nonlinear conversion ratio error corresponding to *Eq.* (8), which is caused by the low parasitic resistance of L (23mΩ). The small slope error is caused by the accuracy of capacitor C, and can be compensated by the V_b.

An example of the captured waveform of the converter operating with conversion ratio V_{OUT}/V_{IN} = 6.5 (V_{IN} = 5V, V_{OUT} = 32V) is shown in *Fig. 18*. In this figure, we can observe the voltage ramp V_C, bias voltage V_b, switch voltage V_{LX} and output voltage V_{OUT}. Here, the dynamics of current source I_b is designed to provide high output impedance (high linearity) in the range 0 - V_b (*i.e* 0 - 500mV). Above, the low supply voltage and parasitic resistance causes the ramp to be nonlinear, what however, has no more impact to the conversion accuracy.

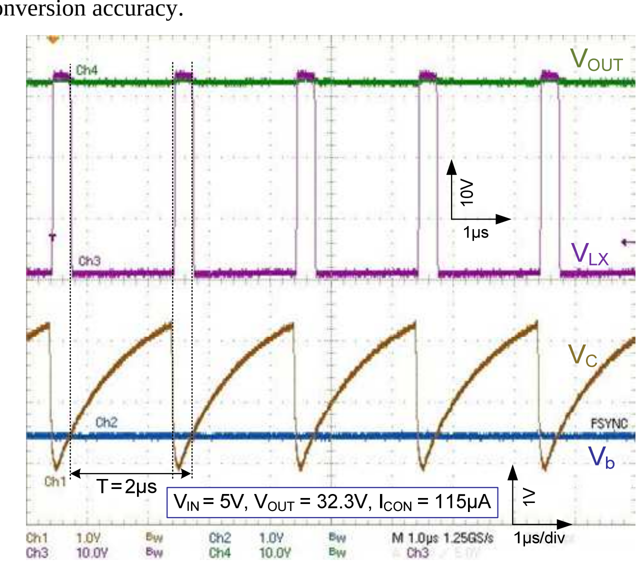

Fig. 18. Measured waveforms of the modulated-ramp PWM generator and power stage with conversion ratio 6.5 (the ramp-linearity error in the range of interest (0-500mV) is < 1%).

Conclusion

The proposed modulated-ramp PWM generator aims to achieve a linear static conversion characteristic for specified switched converters operating in continuous conduction mode (CCM). The obtained linear conversion characteristic enhances the accuracy of the output voltage control. This is very important in the design of the open-loop architecture, where the linearization lowers the sensitivity of control gain at high duty-cycle values. In this paper, analytical models describing static and dynamic behavior of the modulated ramp PWM scheme were delivered, allowing its efficient evaluation, design, and optimization**.**

Acknowledgments

This paper has been prepared with helpful remarks and suggestions of Mr. Sebastien Cliquennois from ST-Ericsson Grenoble. I would like also to thank Mr. Herman Hugo from Infineon technologies (CA) and my future wife Bianca Hugo for the paper form checking and final paper revision.

References

[1] M. K. Kazimierczuk, "*Pulse-width modulated DC-DC power converters,*" Book, John Wiley and Sons Ltd, 2008.

[2] C. Basso, "*Switch mode power supplies: SPICE simulations and practical designs,"* Book, McGraw-Hill 2001.

[3] *"Understanding boost power stages in switchmode power supplies,"* Application report Texas Instrument SLVA061 1999, www.ti.com.

[4] M. K. Kazimierczuk, R. S. Geise, A. Reatti, *"Small-signal analysis of a PWM boost DC-DC converter with a non-symmetric phase integral-lead controller,"* in Proc. of 17th IEEE int. Telecommunications Energy Conference INTELEC, 1995, pp. 608 – 615.

[5] B. Bryant, M.K. Kazimierczuk, "*Voltage loop of boost PWM DC-DC converters with peak current-mode control,"* in IEEE Transactions on Circuits and Systems I: Vol. 53 , pp. 99 – 105, 2006.

[6] D. Liebal, P.Vijayraghavan, N.Sreenath, "*Control of DC-DC buck-boost converter using exact linearization techniques,*" in Proc. of IEEE Power Electronics Specialists Conference PESC 1993, pp. 203 - 207.

[7] H. Sira-Ramirez, M. Rios-Bolivar, A.S.I. Zinober, "*Adaptive input-output linearization for PWM regulation of DC-to-DC power converters,"* in Proc. of the American Control Conference, 1995, pp. 81 - 85.

[8] Yu-Kang Lo, Shang-Chin Yen, Jan-Ming Wang, "*Linearization of the control-to-output transfer function for a PWM buck-boost converter,"* in proc. IEEE International Symposium on Industrial Electronics, 2004, pp. 875 – 877.

[9] J.S. Lin, C.L. Chen, "*Buck/boost servo amplifier for direct-drive-valve actuation*", IEEE Transactions on Aerospace and Electronic Systems, Vol. 31 Issue 3 1995.

[10] M.K. Kazimierczuk, N. Kondrath, "*control-to-output and duty ratio-to-inductor current transfer function of peak current-mode controlled dc-dc PWM buck converter in CCM,*" in proc. of IEEE conf. Circuit and Systems ISCAS, 2010, pp. 2734 - 2737.

[11] Z. Kolka, D. Biolek, J. Kovar, "*On accuracy of averaged control-to-output frequency responses of switched DC-DC converters,"* in proc. of 20th IEEE conference Radioelektronika, 2010, pp. 1 – 4.

[12] V. Vorperian, "*Simplified analysis of PWM converters using the model of the PWM switch, Part I: Continuous conduction mode,*" in IEEE trans. of Aerospace and Electronic Systems, vol.AES-26, pp. 497-505, May 1990.

[13] Qing Wang, Longxing Shi, Changyuan Chang, "*Small-signal transfer functions for a single-switch buck-boost converter in continuous conduction mode,*" in Proc. of Int. Conference on Solid-State and Integrated-Circuit Technology ICSICT 2008, pp. 2016 - 2019.

[14] D.Biolek, V. Biolkova, Z. Kolka. "*Averaged modeling of switched DC-DC converters based on spice models of semiconductor switches,"* in proc. of CSECS'08, the 7th WSEAS Int. Conference on Circuits, Systems, Electronics, Control and Signal Processing, Tenerife, Spain, 2008.

[15] P. H. Forghani-zadeh, G.A.Rincon-Mora, "*Current-sensing techniques for DC-DC converters,*" in proc. of 45th symposium on Circuit and Systems MWCAS 2002. pp. II-557 – II-580.

[16] P. Horowitz, W. Hill, "The Art of Electronic", book, Cambridge University Press New York, 1989.

[17] C. Toumazou, "*Analogue Ic design: the current-mode approach,"* book IEE Circuit and Systems, 1990.

[18] D.G. Holmes,T. A. Lipo, "Pulse width modulation for power converters: principles and practice", Wiley-IEEE Press, October 2003.

[19] V. Michal, C. Premont, G. Pillonnet, N. Abouchi, "*Single active element PID controllers,*" IEEE proc of 20th International Conference Radioelektronika 2010.

[20] R.L. Ford, F.E.J Giring, "*Active filters and oscillators using simulated inductance*," Electronics Letters, Volume: 2, Issue: 2 1966.

Vratislav Michal was born in Olomouc, Czech Republic, in 1980. He received the M.S. degree in electrical engineering and control from the Brno University of Technology, Brno, Czech Republic, in 2004, and the Ph.D. degree in microelectronics from Supelec, Universit´e Pierre et Marie Curie, Paris, France. He joined ST-Ericsson, Grenoble, France, in 2008 as a Postdoctoral Researcher with L'Ecole Superieur de Chimie, Physique and Electronique de Lyon, and since 2010 he is a full-time research and IC Design Engineer.

He is involved in the research and design of switchedmode power converters for mobile phones and tablet platforms. Past and present research activities concern mainly circuit theory, analog signal processing with a particular focus on the analog frequency filters, optimization of switched DC/DC converters, and activity on cryogenic electronic as the ultralow temperature amplifiers and superconducting rapid single flux quantum logic. Dr. Vratislav Michal received several awards as an early-stage researcher from the Czech Ministry of Education, Brno University of Technology, and Czech Radio Club.